Ann. Occup. Hyg., Vol. 57, No. 7, pp. 884–897, 2013
© The Author 2013. Published by Oxford University Press on behalf of the British Occupational Hygiene Society
doi:10.1093/annhyg/met014

Laboratory Evaluation of the Particle Size Effect on the Performance of an Elastomeric Half-mask Respirator against Ultrafine Combustion Particles

XINJIAN HE[1], SERGEY A. GRINSHPUN[1]*, TIINA REPONEN[1], MICHAEL YERMAKOV[1], ROY MCKAY[1], HIROKI HARUTA[2] and KAZUSHI KIMURA[2]

[1]Center for Health-Related Aerosol Studies, Department of Environmental Health, University of Cincinnati, PO Box 670056, Cincinnati, OH 45267-0056, USA; [2]Koken Ltd, 7 Yonbancho, Chiyoda-ku, Tokyo 102–8459, Japan

Received 9 December 2012; in final form 1 February 2013; Advance Access publication 19 April 2013

Objectives: This study quantified the particle size effect on the performance of elastomeric half-mask respirators, which are widely used by firefighters and first responders exposed to combustion aerosols.

Methods: One type of elastomeric half-mask respirator equipped with two P-100 filters was donned on a breathing manikin while challenged with three combustion aerosols (originated by burning wood, paper, and plastic). Testing was conducted with respirators that were fully sealed, partially sealed (nose area only), or unsealed to the face of a breathing manikin to simulate different faceseal leakages. Three cyclic flows with mean inspiratory flow (MIF) rates of 30, 85, and 135 L/min were tested for each combination of sealing condition and combustion material. Additional testing was performed with plastic combustion particles at other cyclic and constant flows. Particle penetration was determined by measuring particle number concentrations inside and outside the respirator with size ranges from 20 to 200 nm.

Results: Breathing flow rate, particle size, and combustion material all had significant effects on the performance of the respirator. For the partially sealed and unsealed respirators, the penetration through the faceseal leakage reached maximum at particle sizes >100 nm when challenged with plastic aerosol, whereas no clear peaks were observed for wood and paper aerosols. The particles aerosolized by burning plastic penetrated more readily into the unsealed half-mask than those aerosolized by the combustion of wood and paper. The difference may be attributed to the fact that plastic combustion particles differ from wood and paper particles by physical characteristics such as charge, shape, and density. For the partially sealed respirator, the highest penetration values were obtained at MIF = 85 L/min. The unsealed respirator had approximately 10-fold greater penetration than the one partially sealed around the bridge of the nose, which indicates that the nose area was the primary leak site.

Keywords: combustion aerosol; half-mask; manikin; particle size; penetration; respirator fit

INTRODUCTION

The US Bureau of Labor Statistics (BLS) has reported that firefighting ranks among the most dangerous occupations in the USA (BLS, 2003). Firefighters are known to have respiratory problems due to smoke inhalation resulting from combustion (Musk et al., 1982; Materna et al., 1992; CDC, 2006). First responders as well as other workers exposed to combustion aerosols are at a similar health risks as firefighters, although their associated health effects are not as well documented. Smoke generated from a fire consists

*Author to whom correspondence should be addressed: Tel: 1-513-558-0504; Fax: 1-513-558-2263; e-mail: sergey.grinshpun@uc.edu

Downloaded from http://annhyg.oxfordjournals.org/ at CDC Public Health Library & Information Center on March 26, 2014

primarily of fine (≤ 1 μm) and ultrafine (≤ 0.1 μm) particles. These smoke particles contain a variety of reactive free radicals and other chemical compounds, which pose a potential health risk (Leonard et al., 2007). Baxter et al. (2010) reported >70% (by number) of smoke particles present during fire knockdown and overhaul are ultrafine. With an increase in surface area, ultrafine particles can be toxicologically more reactive than those of larger sizes (Lam et al., 2004; Shvedova et al., 2005).

During fire overhaul (after the fire has been extinguished), firefighters enter the structure to examine areas for possible re-ignition. At that stage, it has been reported that firefighters may use elastomeric half-mask respirators equipped with a highly efficient P-100 filters (Bolstad-Johnson et al., 2000; Burgess et al., 2001). When subjected to the National Institute for Occupational Safety and Health (NIOSH) respirator certification test, a P-100 filter must provide at least a 99.97% efficiency when challenged to polydisperse dioctyl phthalate (DOP) particles having a count median diameter (CMD) of 185 ± 20 nm and a geometric standard deviation (GSD) of <1.60 (Shaffer and Rengasamy, 2009).

Numerous studies have been conducted to determine the filter efficiency of commercially available respirators (Martin and Moyer, 2000; Eninger et al., 2008; Eshbaugh et al., 2009; Rengasamy et al., 2008; Rengasamy et al., 2009). However, the respirator performance is affected not only by the filter efficiency but also by the faceseal leakage. Furthermore, several studies have shown that particle penetration through the faceseal leakage may be much higher than through the filter medium (Coffey et al., 1998; Zhuang et al., 1998; Grinshpun et al., 2009; Cho et al., 2010b). To account for these two penetration pathways, NIOSH has proposed the total inward leakage (TIL) method for testing respirators (NIOSH, 2009). However, the NIOSH TIL test does not consider particle size, as it is based on non–size selective measurement. TIL was investigated as a function of particle size (aerodynamic size: 0.04–1.3 μm) in our previous research performed with N95 respirators and surgical masks (Lee et al., 2008). The lowest protection factors (PFs) were observed in the size range of 0.04–0.2 μm (which includes the ultrafine fraction). Faceseal leaks on one brand of half-mask respirator (US Safety Series 200 Half-mask) worn by 73 subjects were studied by Oestenstad and Perkins (1992). They found respirator leakage was strongly affected by leaks at the nose and chin, and consideration should be given to including nasal dimensions when selecting a respirator for an individual wearer. Our recent study with a half-mask respirator tested on a breathing manikin revealed that the nose was the primary leak site (He et al., 2013).

There are no data available about the ultrafine particle penetration through faceseal leaks of elastomeric respirators even for a relatively simple case when the breathing flow rate is assumed to be constant. It is much more complex to quantify the particle penetration under actual breathing conditions (when the air flow through a respirator is not constant but has a cyclic nature). Early researchers addressed the effects of faceseal leakage on the particle penetration (Hinds and Kraske, 1987; Chen et al., 1990; Chen and Willeke, 1992). A recent study conducted by Rengasamy and Eimer (2011) investigated the TIL of nanoparticles through Filtering Facepiece Respirators (FFRs) and reported that penetration increased with increasing leak size. With smaller size leaks (< 1.65 mm), the penetration values measured for 50 nm size particles were ~2-fold higher than the values determined for 8 and 400 nm size particles. However, the quoted studies were conducted using either constant flow or artificially induced leaks. Cho et al. (2010b) investigated a more realistic faceseal leakage by partially sealing a N95 respirator on a manikin face with breathing patterns simulated (as a sinusoidal function) by a breathing simulator. That paper showed that most of particles penetrated into the respirator through the faceseal leakage, rather than through the filter. A similar conclusion was drawn by Grinshpun et al. (2009) for a N95 FFR and a surgical mask.

Different challenge aerosols (non-biological and biological) have been utilized for various respiratory protection research including NaCl, Ag, DOP, and viruses (enterobacteriophages MS2, T4, and Bacillus subtilis phage) (Balazy et al., 2006a; Huang et al., 2007; Eninger et al., 2008; Shaffer and Rengasamy, 2009; Cho et al., 2010a; Rengasamy and Eimer, 2011). In most of the previous respirator evaluation studies the challenge aerosol was charge neutralized/equilibrated. To our knowledge, besides our latest investigation (He et al., 2013), no peer-reviewed published study has yet reported respirator performance using combustion aerosols that likely have different charge, shape, and density.

The present investigation is a follow-up to the study of He et al. (2013) performed with challenge aerosols originating from the combustion of wood, paper, and plastic. Similar to our earlier

Downloaded from http://annhyg.oxfordjournals.org/ at CDC Public Health Library & Information Center on March 26, 2014

study, the present investigation aims at testing the performance of an elastomeric half-mask respirator; however, a distinct difference is that the current experimental design includes particle size as an independent variable. Accordingly, a particle size selective measurement technique was deployed in this effort to characterize the effect of particle size along with other factors such as inhalation flow, combustion material, and faceseal leakage on the efficiency of a half-mask respirator.

MATERIALS AND METHODS

Respirator and challenge aerosols

In this study an elastomeric half-mask respirator was tested, which is widely used by firefighters during fire overhaul. This type of respirator is also commonly used by first responders and other workers exposed to combustion aerosols. The model selection was also influenced by feedback from the Cincinnati Fire Department, which indicated that their firefighters frequently wear elastomeric 3M 6000 series half-mask respirators with P-100 filters for medical responses and fire overhaul. Based on this rationale, a medium size 3M 6000 series half-mask respirator equipped with two 3M 2091 P-100 filters was chosen for this study. This same make and model was tested in our latest study on the overall (non-particle-size-selective) particle penetration (He et al., 2013).

Three combustion aerosols were generated by burning the following materials inside a test chamber: wood (24 cm BBQ long matches, 1.9 ± 0.5 g), paper (23 cm × 24 cm brown multifold paper towel, 2.1 ± 0.2 g), and plastic (23 cm × 20 cm Ziploc^{TM} sandwich bags, single layer, 1.7 ± 0.3 g). Wood, paper, and plastic were selected to represent common sources of combustion particles in the environments encountered by firefighters and first responders. It is noted that aerosol particles originated by combustion are usually highly charged; unlike many earlier investigations, no charge neutralization or equilibration was conducted in this study in order to preserve the original properties of combustion particles.

Study design and experimental set-up

The experiments were carried out in the University of Cincinnati indoor testing chamber (volume = 24.3 m^3). The experimental set-up is presented in Fig. 1.

In each experiment, the elastomeric half-mask respirator was donned on a breathing manikin and challenged with one of the three test combustion aerosols. Tests were conducted at three cyclic flows, with mean inspiratory flows (MIFs) of 30, 85, and 135 L/min. These flows represent breathing at medium, high, and strenuous workloads (Lafortuna et al., 1984; Anderson et al., 2006). The cyclic breathing was simulated by a Breathing Recording and Simulation System (BRSS, Koken Ltd., Tokyo, Japan). The BRSS consists of an electromechanical drive-cylinder and two air cylinders connected to each other. A sinusoidal air flow is generated as the electromechanical cylinder moves back (inspiratory duration, half a period) and forth (expiratory duration, half a period) (Haruta et al., 2008). The cylinder moving distance simulates the human tidal volume. By adjusting the speed and distance of the cylinder, the breathing frequency was set at 25 breaths/min for all three cyclic flows. Choosing the same breathing frequency for all cyclic flows eliminated frequency as an additional variable from the study design.

To examine the effect of the faceseal leakage on the performance of the respirator, three sealing conditions, namely 'fully sealed', 'partially (nose area) sealed', and 'unsealed', were established. A silicone sealant was applied to the respirator when it was necessary to seal the facepiece to the manikin. The fully sealed condition essentially targeted the efficiency of the P-100 filters installed on the half-mask respirator, assuming no penetration through the exhalation valve. The unsealed and partially sealed conditions permitted evaluation for both penetration pathways: filter penetration and faceseal leakage. Several studies have reported that faceseal leakage occurs mostly in the nose and chin area (Holton et al., 1987; Crutchfield and Park, 1997; Oestenstad et al., 2007; Oestenstad and Bartolucci, 2010). Our previous study (He et al., 2013) showed that there was no significant difference between two conditions 'nose-only sealed' and 'nose & chin sealed' in terms of the penetration level for the same half-mask respirator. Based on this rationale, only one partially sealed condition—a nose area seal—was chosen for this study (the length of the seal was 12.7 cm, which is ~30% of the 40.6 cm total respirator sealing length).

For each combination of the test conditions, the experiment was repeated four times. The particle concentrations outside and inside of the respirator were measured size-selectively using a recently developed Nanoparticle Spectrometer (Model: Nano-ID NPS500, Naneum Ltd., Kent, UK). To sample from inside the respirator, the half-mask was probed between the nose and upper lip of the

Downloaded from http://annhyg.oxfordjournals.org/ at CDC Public Health Library & Information Center on March 26, 2014

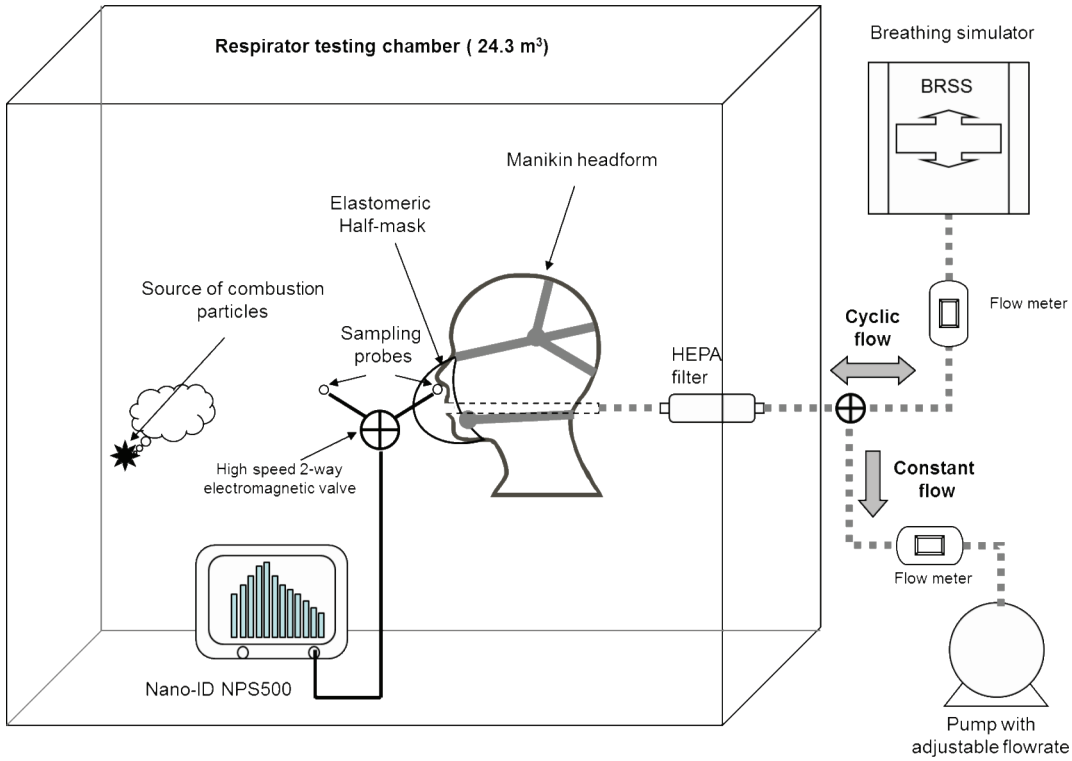

Fig. 1. Schematic diagram of the experimental set-up (modified from He et al., 2013).

manikin using the TSI Model 8025-N95 Fit Test Probe Kit. The Nano-ID is capable of measuring an aerosol particle size distribution over a range of mobility diameters (an equivalent diameter of a spherical particle of the same mobility, Kulkarni et al., 2011) from 5 to 500 nm (referred to as a scan range). The particle counts are recorded in up to 128 user-selectable channels at a sampling flow rate 0.2 L/min, which is sufficiently low (compared with the breathing flow 30–135 L/min) and, therefore, is unlikely to cause significant influence in the measured particle concentration inside the respirator. Myers et al. (1988) stated that biased sampling often occurs because aerosol does not mix well within the respirator cavity during the inhalation phase of the respiratory cycle. To minimize the effect of non-homogeneity of the concentration inside the respirator, resulting from poor mixing, a 3-min scan time was chosen for each measurement; this time allows integrating many cycles in one measurement, e.g. as many as 75 cycles in 3 min at 25 breaths/min.

The particle penetration (through both pathways) was determined for each particle size (d_p) as the ratio of inside and outside concentrations:

$$P(d_p) = \frac{C_{in}}{C_{out}} \times 100\% \quad (1)$$

Data analysis

For each combination of experimental conditions, the mean value of the total penetration and the standard deviation were calculated from the four replicates. One-way analyses of Variance (ANOVA) was performed to quantify the effect of sealing condition on the particle penetration, and three-way ANOVA was used to study the significance of combustion material, breathing flow, and particle size using SAS version 9.2 (SAS Institute Inc., Cary, NC). *P*-values of <0.05 were considered to represent significant differences in the outcomes.

RESULTS AND DISCUSSION

Particle size distribution of challenge combustion aerosols

Fig. 2 shows the particle size distributions of the three combustion aerosols measured at 10, 30, 50, 70, and 90 min after the burning was stopped.

Downloaded from http://annhyg.oxfordjournals.org/ at CDC Public Health Library & Information Center on March 26, 2014

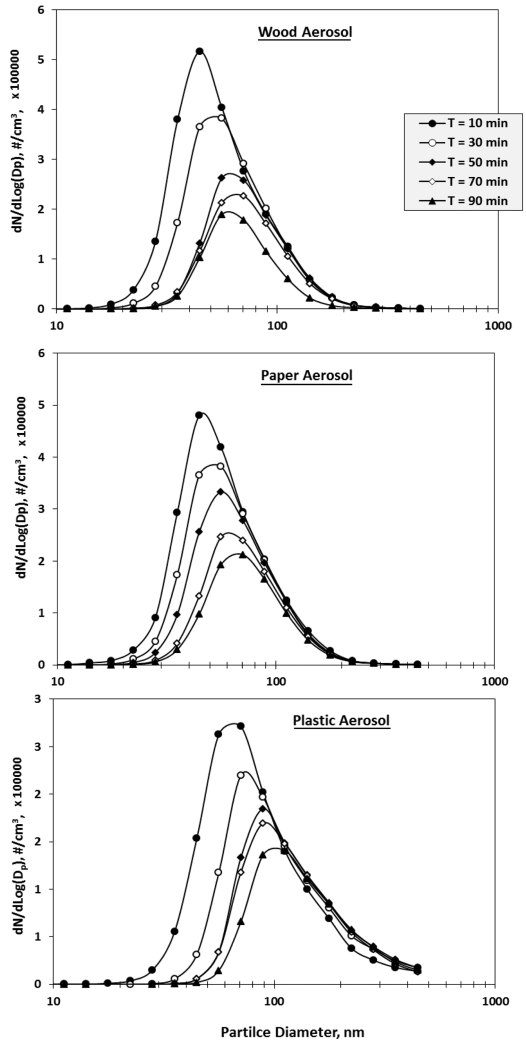

Fig. 2. Particle size distributions of three combustion aerosols (wood, paper, and plastic) measured at 10, 30, 50, 70, and 90 min after the material burning stopped.

Each aerosol produced a single-mode distribution. The peak concentrations occurred in the mobility diameter range of 40–80 nm for wood and paper combustion aerosols, whereas the peaks shifted slightly toward a larger size range (50–100 nm) for plastic combustion aerosols.

The majority of particles detected by the Nanoparticle Spectrometer fell between 20 and 200 nm. This is in a good agreement with the above quoted findings of Baxter et al. (2010), who suggested that the scan range could be narrowed down. In addition to a better representation of the challenge aerosol, a narrower scan range improves the instrument performance in a specific time interval (by providing a more accurate particle count per channel). Accordingly, the size range of 20–200 nm discriminated through 30 scan channels (representing 30 particle size fractions) was selected. The above choice was consistent with an important aim of the particle size selective sampling—to identify the most penetrating particle size (MPPS).

The natural decay of airborne particle concentration was found to be dependent on particle size. It is seen in Fig. 2 that the natural decay was very slow for wood and paper combustion particles >80 nm and plastic combustion particles >100 nm. The slower decay for larger particles can be explained by weakening diffusion as well as continuous coagulation (Kulkarni et al., 2011). The curves demonstrate a pronounced concentration decrease during approximately the first 50 min, which slowed down afterwards. On average, ~40% of particles remained airborne after 90 min. This assured a sufficient number of particles available for counting in each Nano-ID channel.

Fully sealed half-mask respirator with P-100 filters

The fully sealed respirator prevented particles from penetrating through the faceseal leakage. Therefore, total particle penetration equals filter penetration ($P = P_{filter}$), assuming no penetration through the exhalation valve. A separate experiment was conducted to test the assumption that exhalation valve operated properly, thus introducing no additional pathway for particles to penetrate inside the respirator. In this experiment, the same respirator with a functional exhalation valve was compared with a sealed valve. The penetration was determined at a constant flow of 135 L/min as well as at a cyclic flow of MIF=135 L/min. For either flow conditions, no significant difference in the penetration values was found. The results confirmed that the exhalation valve had no influence on particle penetration, which supports the fundamental postulate of our study design of only two particle penetration pathways (filter and faceseal).

Fig. 3 presents the particle penetration values for the fully sealed half-mask respirator equipped with two P-100 filters challenged with particles aerosolized by wood combustion. Our previous study (He et al., 2013) conducted with an identical fully sealed half-mask indicated that the effect of combustion material on the particle penetration was not significant (*P*-value >0.05); therefore, only one combustion material (wood) was tested here. Except

Downloaded from http://annhyg.oxfordjournals.org/ at CDC Public Health Library & Information Center on March 26, 2014

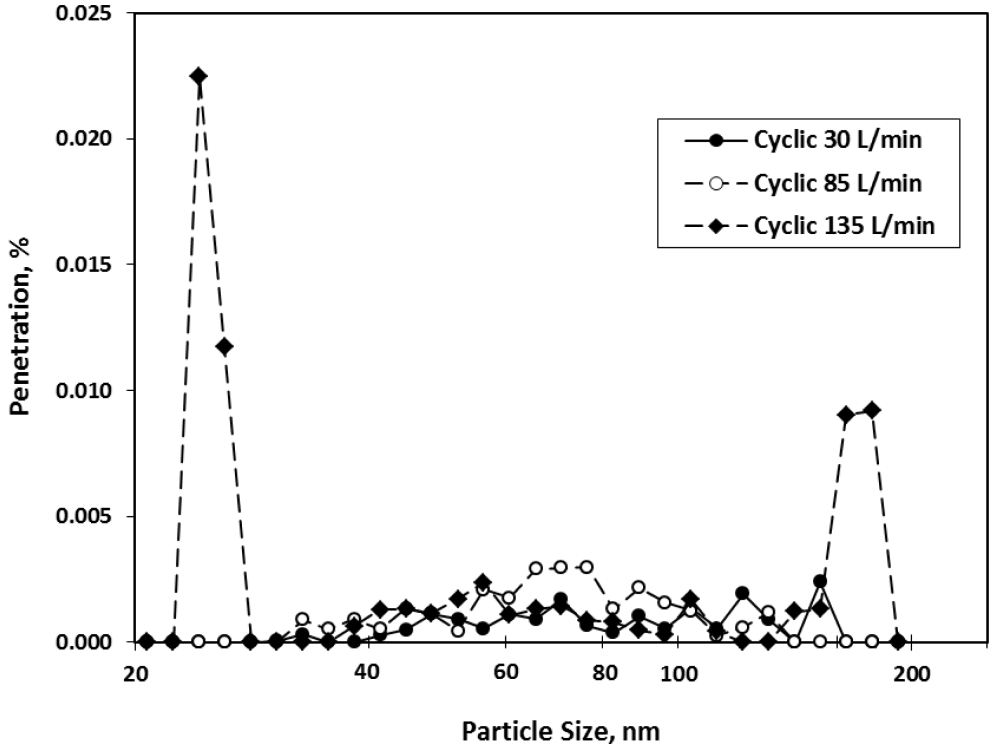

Fig. 3. Penetration of 'wood' combustion aerosol through a fully sealed half-mask equipped with two P-100 filters. Each data point represents the average of four replicates.

for a few points obtained at 135 L/min, all the other values were <0.005% regardless of the particle size and flow rate. The two peak points that occurred at the lower (~30 nm) and higher (~180 nm) sizes could be outliers as there were not sufficient number of particles (C_{out} <10 000 particles/channel, C_{in} <1 particle/channel) generated at those two sizes especially after 90-min measurement (see Fig. 2, Wood Aerosol). However, even if these two peaks were considered as valid data points, the maximum filter penetration would still fall <0.025% (Fig. 3). Overall, the results demonstrate that the tested P-100 filters exhibited the efficiency levels exceeding the NIOSH certification requirement (P ≤0.03%). This finding is in agreement with our earlier results obtained using a non-particle-size-selective aerosol measurement technique (He et al., 2013). Several other studies also reported similarly low particle penetration for P-100 filters (Eshbaugh et al., 2009; Rengasamy and Eimer, 2011).

Partially (nose area) sealed half-mask respirator with P-100 filters

Fig. 4 presents the particle penetration data for partially sealed half-mask with two P-100 filters, which was tested at three MIFs (30, 85, and 135 L/min) while exposed to three combustion aerosols (wood, paper, and plastic). Data analysis revealed that combustion material and particle size had a significant effect on penetration values (P-value < 0.001). For all three materials, the highest particle penetration values occurred at 85 L/min throughout the entire tested particle size range (20–200 nm) except for the first channel; the 135 L/min flow generated the second highest penetration levels followed by 30 L/min. All penetration values obtained with the three combustion aerosols were approximately between 0.05 and 0.7% except a few points obtained for smaller particles at 30 L/min. Insufficient number of particles detected by the Nanoparticle Spectrometer (C_{out} <1000 particles/channel, C_{in} <1 particle/channel) prevented us from reporting penetration values for plastic particles between 20 and ~30 nm (see Fig. 2, Plastic Aerosol).

Compared with the fully sealed test condition, even the lowest penetration values obtained for the partially sealed half-mask at 30 L/min were at least 10-fold greater, regardless of flow rates (30, 85, and 135 L/min). This shows that any additional

Downloaded from http://annhyg.oxfordjournals.org/ at CDC Public Health Library & Information Center on March 26, 2014

faceseal leakage can substantially compromise the protection offered by a half-mask respirator.

The penetration curves obtained for wood and paper combustion aerosols were of similar shapes. While not perfectly monotonic, the curves showed an overall increase of penetration with increasing particle size. For plastic combustion particles, the curves are slightly different from those found for wood and paper aerosols with the penetration reaching the maximum approximately at 120–160 nm at 85 and 135 L/min. One possible reason is that wood and paper combustion aerosol particles are expected to have similar physical and chemical properties while the particles originated by burning plastic, a synthetic material, may differ in composition and physical characteristics such as a charge, shape, and density. It is worth of mentioning that, although effects associated with electrical charges on particles as well as on respirator and manikin surfaces fell outside of the scope of this study, electric forces may have a major contribution to the differences associated with combustion material. It is also to be noted that the measurement of particles in this study was based on their electrical mobility (not an aerodynamic diameters), and there are no data, to our knowledge, that would allow establishing a relationship between the two, at least, for the challenge aerosol. All these factors may explain the material-associated differences and similarities observed in our experiments.

The order of curves in Fig. 4 was somewhat unexpected: at the same particle size the penetration increased as the MIF increased from 30 to 85 L/min but then decreased as the flow continued rising from 85 to 135 L/min at MIF. In order to identify the flow rate(s) associated with the maximum particle penetration, four more cyclic flows (50, 70, 100, and 120 L/min) were added to the testing program for the partially sealed half-mask. This additional experiment was conducted using plastic combustion aerosol only. It is believed that the finding would have higher practical significance because plastic aerosol is comparatively more toxic and more health relevant than the ones produced by burning wood or paper (Underwriters Laboratories Inc, 2010). Thus, seven flows (30, 50, 70, 85, 100, 120, and 135 L/min) were tested at the same manikin breathing frequency (25 breaths/min) with four replicates for each flow. The experimental results are presented in Fig. 5. The penetration values are shown for particle sizes of and above of 30 nm (as mentioned earlier, the count of plastic combustion particles <30 nm was insufficient).

Firstly, the curves (upper section of Fig. 5) corresponding to seven different MIFs are similarly non-monotonic. Although the trend is not completely clear for particle diameters up to 40–50 nm, all the curves indicated that penetration increased with increasing particle size up to

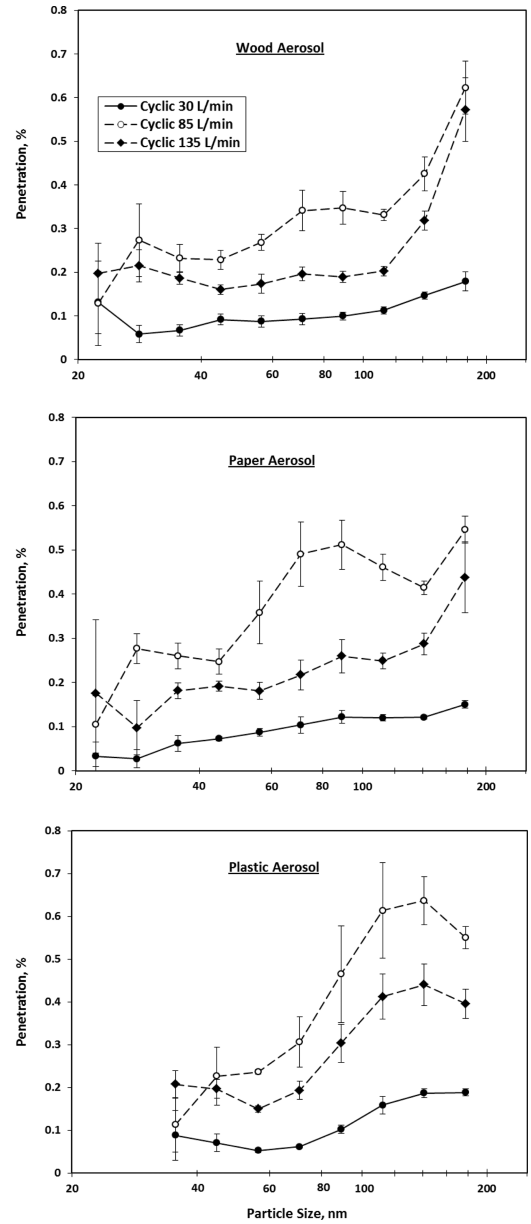

Fig. 4. Penetration of wood, paper, and plastic combustion aerosols through a partially sealed (nose area) half-mask equipped with two P-100 filters. Each point represents the average value of four replicates, and the error bar represents the standard error of the mean.

Downloaded from http://annhyg.oxfordjournals.org/ at CDC Public Health Library & Information Center on March 26, 2014

~100–140 nm (depending on the flow rate) and then decreased for larger particles. The flow rate of 85 L/min indeed appeared to be the one producing the highest penetration values when particle size was >40 nm. The flow rate of 100 L/min produced the second highest penetration (the values are approximately the same compared with 85 L/min in the particle size range of 80 to 100 nm). Further increase in flow rate resulted in decrease in penetration. Results also showed the lowest penetration values at the lowest tested MIF (30 L/min). The following explanations are offered to address the flow effect: as the breathing flow increased from 30 to 85 L/min, more combustion particles were brought into the respirator cavity (greater penetration) while the outside concentration remained unchanged. However, it is anticipated that at higher flows (>85 L/min) the negative pressure inside the respirator during inhalation became sufficiently high to suck the respirator toward the face of the manikin and consequently reduce faceseal leak size. In turn, a smaller leak could correspond to a lower relative contribution of the total air flow entering the facepiece, resulting in penetration of fewer particles. During exhalation, exhaled air is released primarily through the exhalation valve (rather than the faceseal leakage or filters) of the half-mask respirator so that a higher flow should not substantially increase the leak size during exhalation.

Secondly, the lower section of Fig. 5 shows the particle penetration as a function of MIF at four particle sizes (52, 83, 104 and 153 nm) that were selected to fairly represent the entire scan range. This figure conveys that the particle penetration was largely dependent on the cyclic breathing flow, with the highest penetration values occurred at the MIF = 85 L/min. As particle size increased from 52 nm to 104 nm, the penetration values showed a clear increasing trend regardless of the flow rate. However, penetration values obtained at the larger particle size (153 nm) were close to or higher than those acquired at 104 nm (depending on the flow rate). This indicates that the MPPS for this partially sealed half-mask (nose area only) was within a size range of ~100 to 160 nm when challenged to plastic combustion aerosols.

Unsealed half-mask respirator with P-100 filters

The findings for the unsealed half-mask are presented in Fig. 6. The ANOVA results showed that both particle size and material type had strong significant effects (P-value < 0.001) on the particle penetration. The penetration values ranged from 4 to 8% for wood aerosol, from 3 to 10% for paper aerosol, and from 3 to 16% for plastic aerosol. Plastic aerosol produced higher penetration values for particles between 100 and 200 nm compared with wood and paper combustion aerosols. This finding is important in light of previously published evidence that combustion of plastic generates toxic particles that may be associated with human health effects (Linak et al., 1989; Wong et al., 2007).

The average penetration of the unsealed half-mask respirator exceeded that of fully sealed respirator by a factor of >100, given that most of penetration values obtained for the fully sealed half-mask were <0.05% (see Fig. 3). Therefore, more than 99% of particles entering the unsealed half-mask respirator cavity penetrated through faceseal leakage (not through the P-100 filter medium). This finding is consistent with the conclusions presented in He et al. (2013) for the same type of respirator based on total particle concentration measurement (non-size selective).

For plastic aerosol, the size of particles most readily penetrating through faceseal leakage fell in a range of 120–140 nm for all three MIFs, whereas it is difficult to determine the MPPS for wood and paper aerosols as the penetration curves do not show clear peaks in the particle size range of 20–200 nm. Many previous studies on respirator filter efficiency have reported the MPPS for tested filters (Brown, 1993; Martin and Moyer, 2000; Grafe et al., 2001; Bałazy et al., 2006a, 2006b; Eninger et al., 2008). However, there are very limited data available on the MPPS for respirator faceseal leakage. Rengasamy and Eimer (2011) reported that the MPPS for a cylindered leak (<1.65 mm diameter) was ~50 nm. It is commonly assumed that size and location of faceseal leakage are constantly changing during breathing, talking, and head/body movement (Myers et al., 1996), which contributes to additional variability when trying to determine the MPPS. Additional challenge is that the MPPS can be affected by aerosol type as shown in this study.

Unlike the fully sealed condition, an unsealed respirator involves two primary particle penetration pathways (filter medium and faceseal leakage). While numerous studies have addressed the effect of breathing flow on the filter efficiency (e.g. increasing flow rate was shown to promote higher penetration of ultrafine particles due to diffusion) (Bałazy et al., 2006a, 2006b; Eninger et al., 2008; Rengasamy and Eimer, 2011), it is less certain how the breathing flow affects

Downloaded from http://annhyg.oxfordjournals.org/ at CDC Public Health Library & Information Center on March 26, 2014

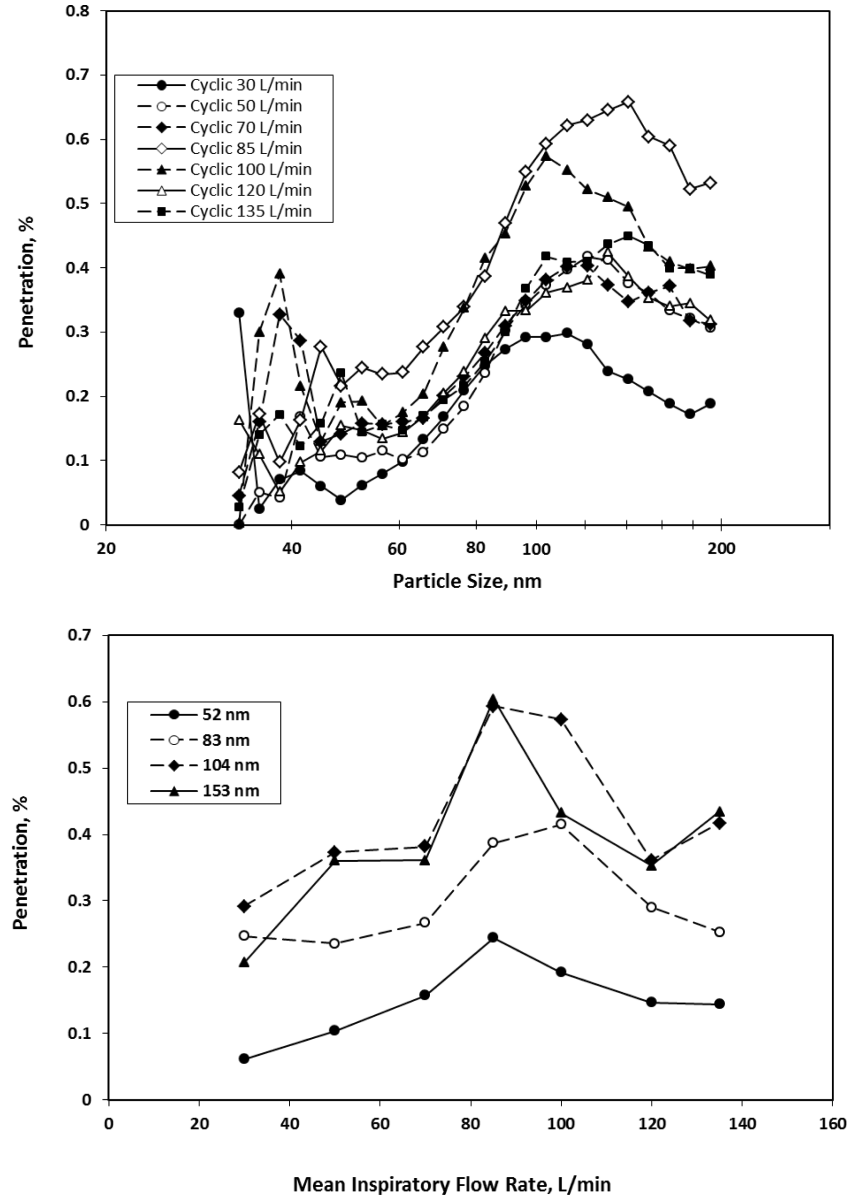

Fig. 5. Penetration of 'plastic' combustion particles through a partially sealed (nose area) half-mask equipped with two P-100 filters: dependence on particle size for fixed MIFs (upper figure) and dependence on the MIF for fixed particle sizes (lower figure). Each point represents the average value of four replicates.

the faceseal penetration. Interestingly, several published FFR studies have documented that faceseal penetration decreased with increase in breathing flow when challenged with particles >500 nm (Chen et al., 1990; Huang et al., 2007; Cho et al., 2010b). On the other hand, another FFR evaluation effort failed to observe significant increase or decrease in faceseal penetration when increasing the breathing flow (Rengasamy and Eimer, 2011) for particles ranging from 8 to 400 nm. In our study, increasing flow seemed to decrease particle penetration through the faceseal leakage, and such effect was most dominant for plastic aerosol and particle size of >100 nm (see Fig. 6). It is acknowledged that our study tested a different respirator (elastomeric half-mask) with different challenge aerosols compared with the three studies referenced above.

Downloaded from http://annhyg.oxfordjournals.org/ at CDC Public Health Library & Information Center on March 26, 2014

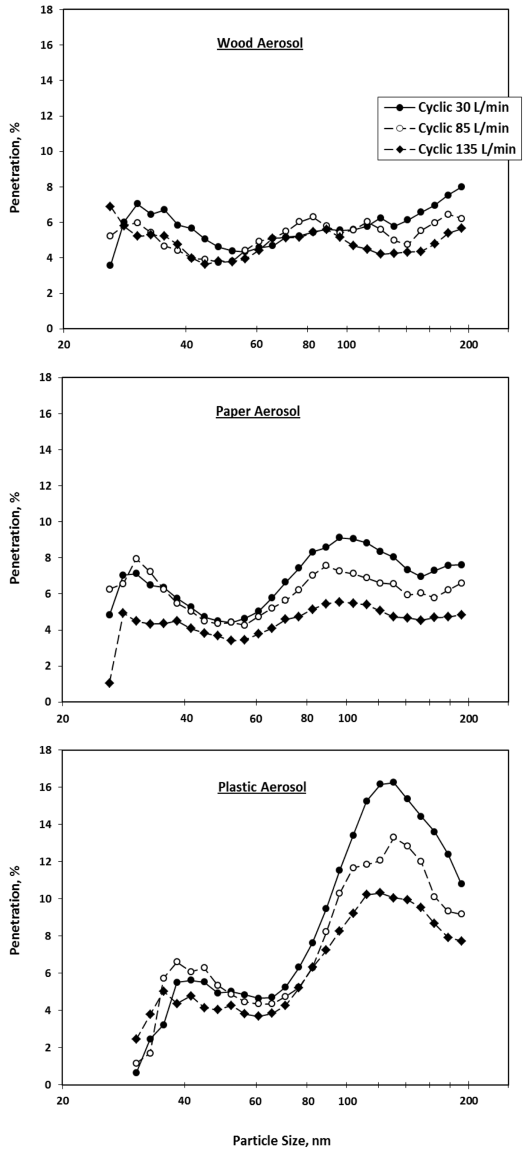

Fig. 6. Penetration of wood, paper, and plastic combustion aerosols through an unsealed half-mask equipped with two P-100 filters. Each point represents the average value of four replicates.

To interpret the above finding (faceseal penetration decreases with increasing flow rate), an experiment with breathing flow held constant was conducted. The same unsealed half-mask was tested using three constant flow rates (30, 85, and 135 L/min) while challenged with plastic aerosol. The results are shown in Fig. 7. First, constant inhalation flow produced much higher penetration values than cyclic flow. Peak penetration was close to 50% for a constant flow rate of 30 L/min (Fig. 7) compared with 16% for cyclic flow of the same MIF (Fig. 6); similar trends were observed for 85 and 135 L/min. These differences were explained in our previous study (He et al., 2013). The important finding is that increasing constant flow was generally associated with a decrease in particle penetration (with the exception of data obtained at 85 versus 135 L/min for larger particles). Due to the high efficiency of the P-100 filter, the total particle penetration through the half-mask elastomeric respirator is almost fully determined by the number of particles penetrating through faceseal leakage. Most of tested particles are small enough to have their motion governed primarily by diffusion and electrostatics. Assuming that (a) the exhalation valve provides a perfect seal, (b) the particle loss inside the faceseal leakage is negligibly small, and (c) the capture efficiency of the P-100 filter is close to 100%; the total particle penetration (P_{Total}) into a respirator is determined by the relative contributions of the air flows through the filter and the leakage (He et al., 2013):

$$P_{Total} \approx 1 - \frac{Q_F}{Q} = \frac{Q_L}{Q} \times 100\% \qquad (2)$$

Where Q_F is the constant air flow through filter media, Q_L is the constant air flow through faceseal leakage, and $Q = Q_F + Q_L$ is the constant total flow. If the respirator is equipped with an absolute filter, the penetration value calculated by equation (2) can be considered as maximum possible particle penetration.

Depending on the position of the respirator and the tightness of the straps, the gap between the respirator and the face of the manikin is likely variable. In our experiment, the most sizeable leakage (~1 mm) was observed around the nose area. However, in areas around the chin and cheeks the faceseal leakage could be 0.1 mm or lower. According to the classic particle diffusion theory (Kulkarni et al., 2011), the particle losses inside a 1-mm gap are estimated to be negligibly low (with the Brownian displacement of ~0.01 mm). At the same time, the diffusional deposition inside a 0.1 mm gap is not negligible, especially for particles below ~50 nm. Larger particles (well above 50 nm) are not subjected to appreciable diffusional deposition, but some of them may carry substantial electrical charges, which could cause losses inside the faceseal leakage and consequently decrease the particle penetration. This

Downloaded from http://annhyg.oxfordjournals.org/ at CDC Public Health Library & Information Center on March 26, 2014

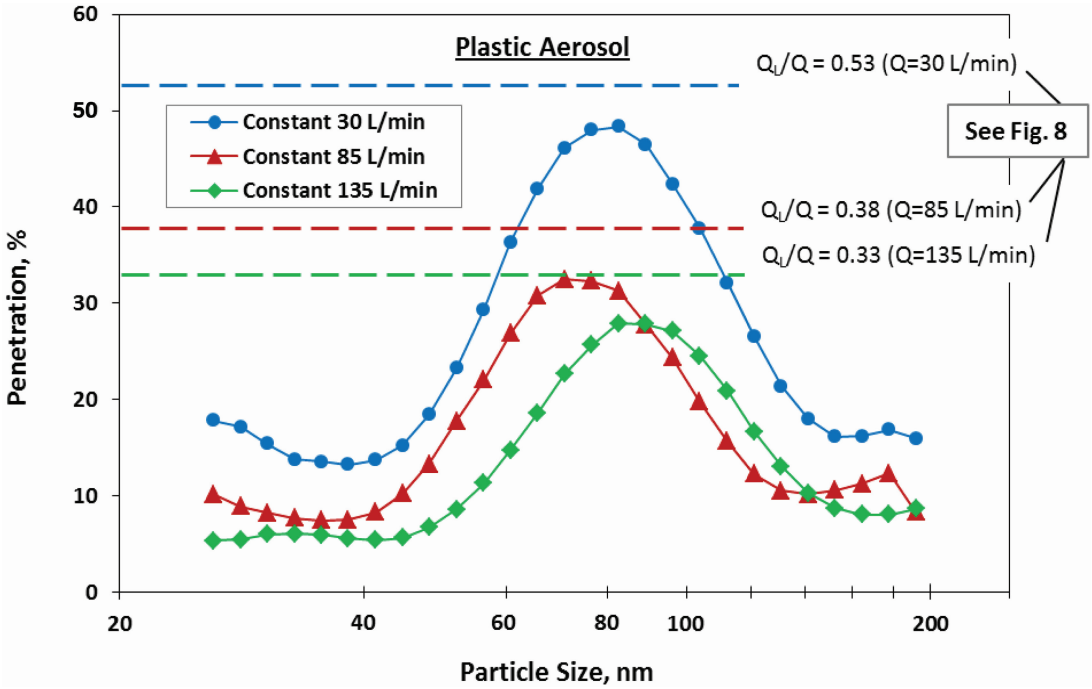

Fig. 7. Penetration of the plastic combustion aerosol through an unsealed half-mask equipped with two P-100 filters under constant flow regime. Each point represents the average value of four replicates. Additionally, the graph shows three straight dotted lines representing Q_L/Q values at Q = 30, 85, and 135 L/min, which correspond to the maximum particle penetrations at these flow rates, as determined from Fig. 8.

effect is expected to be more pronounced as the particle size increases (further increase of the particle size adds interception and impaction losses). The above explains the non-monotonic curves shown in Fig. 7. The MPPSs ranging ~70–90 nm (depending on the flow rate) represent the condition when the particles are too large for substantial diffusional losses inside the leakage but at the same time too small to expect notable deposition due to electrostatic mechanism, interception, and impaction. In these cases, the penetration is close to the theoretically maximum level, Q_L/Q [Eq. (2)]. These thresholds are shown in Fig. 7 for each of the three flow rates as straight lines.

The proportion of total flow through the faceseal leakage was experimentally determined for an unsealed half-mask donned on the manikin under the constant flow condition. This was done as follows. First, the respirator was fully sealed on the manikin, and the air flow was established (entirely through the filter in absence of the faceseal leakage). By adjusting the speed of a vacuum pump, seven constant flow rates (Q_F) ranging from 10 to 100 L/min were achieved and the seven corresponding static pressures (pressure drop) were recorded. Second, an unsealed respirator was donned on the manikin with both P-100 filters removed and all inhalation openings fully covered to allow the air pass solely through the leakage. Using the same pre-recorded static pressures, seven flow rates (Q_L) were established by adjusting the vacuum pump. Subsequently, the seven total flow rates were calculated ($Q = Q_F + Q_L$, see Fig. 8 for the seven tested Q-values marked as black dots).

The relationship between Q_L/Q and total flow Q is plotted in Fig. 8. The graph reveals that Q_L/Q values decreased along with increasing total flow rate. As indicated above, this likely occurred due to high negative pressure inside of the respirator that sucks it towards the manikin surface, thus reducing the faceseal leakage and producing higher flow resistance, which, in turn, reduced the proportion of total flow (Q_L/Q) passing through the leakage. Increase in total flow decreased the slope of the curve shown in Fig. 8. At a total flow of 30 L/min, the ratio of Q_L/Q was as high as 53%, which, based on our theoretical considerations presented above, was

Downloaded from http://annhyg.oxfordjournals.org/ at CDC Public Health Library & Information Center on March 26, 2014

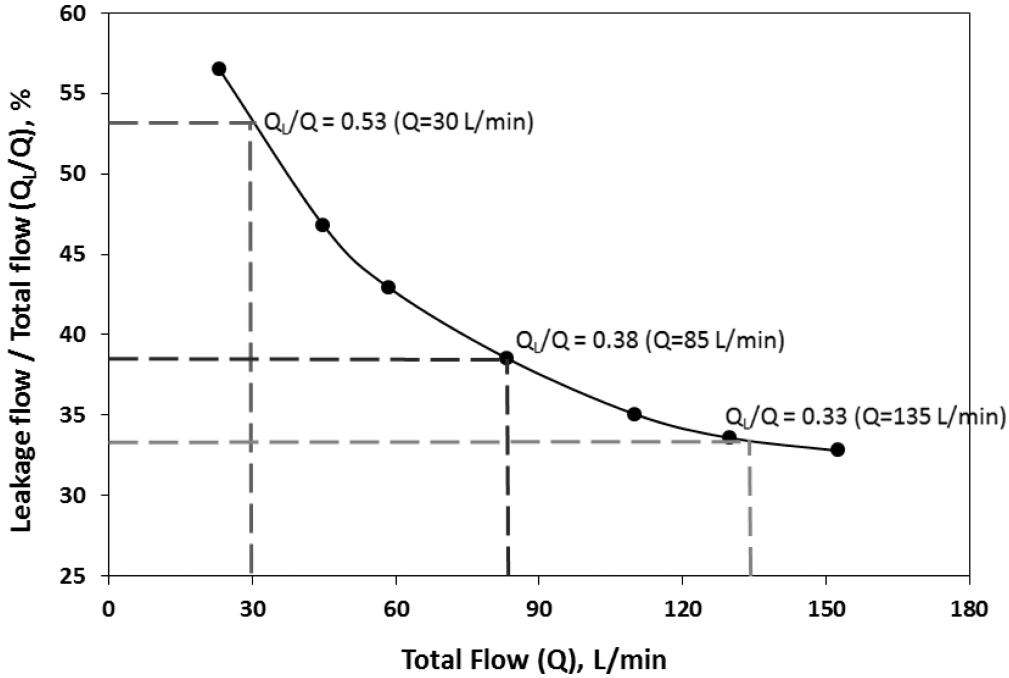

Fig. 8. The relationship between the leakage-portion of total flow (Q_L/Q) and the total flow (Q) under constant flow regime. Each black dot represents the flow measurement for a certain static pressure. The dotted lines represent Q_L/Q values at Q = 30, 85, and 135 L/min.

supposed to produce $P_{Total} \approx Q_L/Q = 53\%$ (see Fig. 7, the 53% straight line). Similarly, when the total flow was 85 and 135 L/min, the Q_L/Q was 38 and 33%, respectively.

The above explanations can be applied to a more complex case of the cyclic flow regime, which—in contrast to the constant flow—exhibits both inhalation and exhalation. During exhalation, particle concentration inside the respirator is diluted by the purified exhalation air (in our experimental set-up, a HEPA filter installed between the manikin and the breathing simulator). At the same time, the particles cannot be entirely removed from the respirator cavity as there are always particles trapped inside the respirator after exhalation. Thus, the particle penetration obtained under the cyclic flow regime is expected to be lower than those obtained under the constant flow regime (see a more detailed explanation in He et al., 2013). However, the effects of the flow rate on the faceseal penetration remained the same for both constant flow and cyclic flow regimes—higher flow associated with lower penetration, which was proven by the theoretical calculation [equation (2)] combined with the flow measurements (Fig. 8). No previously published studies were found to address the flow type (cyclic versus constant) effect on the total inward leakage for the elastomeric half-masks.

CONCLUSIONS

Performance of the elastomeric half-mask respirator was significantly affected by the particle size (P-value < 0.001). When testing the partially sealed half-mask, the highest penetration was detected at 180 nm for wood and paper combustion aerosols and at ~120–160 nm for plastic aerosol. Under the unsealed conditions, the peak penetration occurred at 120 nm for plastic combustion aerosol, while no clear peaks were identified for wood and paper. Results suggest that the MPPS for the faceseal leakage was >100 nm for the partially sealed and unsealed conditions when challenged with plastic aerosol. The partially sealed (nose area only) half-mask respirator resulted in 10-fold lower penetration levels when compared with the unsealed condition. This suggests that the nose area was a primary leak site.

Material type was another significant factor (P-value < 0.001). For the unsealed half-mask challenged with plastic combustion aerosol, higher penetration values were observed compared with wood and paper aerosols for particles >100 nm.

Downloaded from http://annhyg.oxfordjournals.org/ at CDC Public Health Library & Information Center on March 26, 2014

The effect of cyclic flow rate was found to be significant as well (P-value < 0.001). For the partially sealed respirator, increasing flow rate was associated with an increase in penetration up to MIF = 85 L/min. For higher flow rates, the trend changed to a decrease in penetration as the flow increased. For unsealed conditions, increasing flow rate resulted in consistent decrease of penetration and this trend was most apparent for the plastic aerosol with size >100 nm.

One major limitation of this study is that a hard plastic manikin headform was used, which was not capable of mimicking the texture and softness of human skin. This may potentially create larger leaks for equivalent strap tension. An advanced headform covered with soft skin-like material may be considered as an appropriate alternative in future studies. Only one model of the elastomeric half-mask was tested, which also represents a study limitation. Additionally, it is acknowledged that all the cyclic flows tested in this study used the same breathing frequency (25 breaths/min), which may not fully represent the real-world situation. Future studies are needed to investigate the effects of the breathing frequency on the performance of respiratory protection devices.

FUNDING

NIOSH Targeted Research Training program of the University of Cincinnati Education and Research Center grant (No.T42/OH008432-06) and the University of Cincinnati Graduate Assistantship and Scholarship.

REFERENCES

Anderson NJ, Cassidy PE, Janssen LL, Dengel DR. (2006) Peak Inspiratory Flows of Adults Exercising at Light, Moderate and Heavy Work Loads. J. Int. Soc. Res. Prot; 23: 53–63.

Balazy A, Toivola M, Adhikari A *et al.* (2006a) Do N95 respirators provide 95% protection level against airborne viruses, and how adequate are surgical masks? Am J Infect Control; 34: 51–7.

Balazy A, Toivola M, Reponen T *et al.* (2006b) Manikin-based performance evaluation of N95 filtering-facepiece respirators challenged with nanoparticles. Ann Occup Hyg; 50: 259–69.

Baxter CS, Ross CS, Fabian T *et al.* (2010) Ultrafine particle exposure during fire suppression–is it an important contributory factor for coronary heart disease in firefighters? J Occup Environ Med; 52: 791–6.

BLS. (2003) Occupational Injuries and Illnesses in the US by Industry International Association of Firefighters. Washington, DC: US Bureau of Labor Statistics. 1995–1996.

Bolstad-Johnson DM, Burgess JL, Crutchfield CD *et al.* (2000) Characterization of firefighter exposures during fire overhaul. AIHAJ; 61: 636–41.

Brown RC. (1993) Air filtration: An integrated approach to the theory and applications of fibrous filters. Oxford: Pergamon Press. p.109. ISBN: 0080412742.

Burgess JL, Nanson CJ, Bolstad-Johnson DM *et al.* (2001) Adverse respiratory effects following overhaul in firefighters. J Occup Environ Med; 43: 467–73.

CDC. (2006) Fatalities among volunteer and career firefighters—United States, 1994–2004. The Journal of the American Medical Association; 295: 2594–96.

Chen CC, Ruuskanen J, Pilacinski W *et al.* (1990) Filter and leak penetration characteristics of a dust and mist filtering facepiece. Am Ind Hyg Assoc J; 51: 632–9.

Chen CC, Willeke K. (1992) Characteristics of face seal leakage in filtering facepieces. Am Ind Hyg Assoc J; 53: 533–9.

Cho KJ, Jones S, Jones G *et al.* (2010a) Effect of particle size on respiratory protection provided by two types of N95 respirators used in agricultural settings. J Occup Environ Hyg; 7: 622–7.

Cho KJ, Reponen T, McKay R *et al.* (2010b) Large particle penetration through N95 respirator filters and facepiece leaks with cyclic flow. Ann Occup Hyg; 54: 68–77.

Coffey CC, Zhuang Z, Campbell, D.L. Myers, W.R. (1998) Quantitative fit testing of N95 respirators: part II - results, effect of filter penetration, fit test, and pass/fail criteria. J Int Soc Res Prot; 16(1–4): 25–36.

Crutchfield CD, Park DL. (1997) Effect of leak location on measured respirator fit. Am Ind Hyg Assoc J; 58: 413–7.

Eninger RM, Honda T, Adhikari A *et al.* (2008) Filter performance of n99 and n95 facepiece respirators against viruses and ultrafine particles. Ann Occup Hyg; 52: 385–96.

Eshbaugh JP, Gardner PD, Richardson AW *et al.* (2009) N95 and p100 respirator filter efficiency under high constant and cyclic flow. J Occup Environ Hyg; 6: 52–61.

Grafe T, Gogins M, Barris M, Schaefer J, Canepa R. (2001) "Nanofibers in Filtration Applications in Transportation". Filtration 2001 Conference Proceedings. Chicago, IL, pp 1–15.

Grinshpun SA, Haruta H, Eninger RM *et al.* (2009) Performance of an N95 filtering facepiece particulate respirator and a surgical mask during human breathing: two pathways for particle penetration. J Occup Environ Hyg; 6: 593–603.

Haruta H, Honda T, Eninger RM, Reponen T, McKay R, Grinshpun SA. (2008) Experimental and theoretical investigation of the performance of N95 respirator filters against ultrafine aerosol particles tested at constant and cyclic flows. J Int Soc Res Prot; 25: 75–88.

He X, Yermakov M, Reponen T, McKay R, James K, Grinshpun SA. (2013) Manikin-based performance evaluation of elastomeric respirators against combustion particles. J Environ Occup Hyg; 10: 203–12.

Hinds WC, Kraske G. (1987) Performance of dust respirators with facial seal leaks: I. Experimental. Am Ind Hyg Assoc J; 48: 836–41.

Holton PM, Tackett DL, Willeke K. (1987) Particle size-dependent leakage and losses of aerosols in respirators. Am Ind Hyg Assoc J; 48: 848–54.

Huang S-H, Chen C-W, Chang C-P, Lai C-Y, Chen C-C. (2007) Penetration of 4.5 nm to aerosol particles through fibrous filters. J Aerosol Sci; 38: 719–27.

Downloaded from http://annhyg.oxfordjournals.org/ at CDC Public Health Library & Information Center on March 26, 2014

Kulkarni P, Baron PA, Willeke K. (2011) Aerosol Measurement - Principles, Techniques, and Applications. 3rd edn. New Jersey: John Wiley & Sons.

Lafortuna CL, Minetti AE, Mognoni P. (1984) Inspiratory flow pattern in humans. J Appl Physiol; 57: 1111–9.

Lam CW, James JT, McCluskey R *et al.* (2004) Pulmonary toxicity of single-wall carbon nanotubes in mice 7 and 90 days after intratracheal instillation. Toxicol Sci; 77: 126–34.

Lee SA, Grinshpun SA, Reponen T. (2008) Respiratory performance offered by N95 respirators and surgical masks: human subject evaluation with NaCl aerosol representing bacterial and viral particle size range. Ann Occup Hyg; 52: 177–85.

Leonard SS, Castranova V, Chen BT *et al.* (2007) Particle size-dependent radical generation from wildland fire smoke. Toxicology; 236: 103–13.

Linak WP, Ryan JV, Perry E *et al.* (1989) Chemical and biological characterization of products of incomplete combustion from the simulated field burning of agricultural plastic. JAPCA; 39: 836–46.

Martin SB Jr, Moyer ES. (2000) Electrostatic respirator filter media: filter efficiency and most penetrating particle size effects. Appl Occup Environ Hyg; 15: 609–17.

Materna BL, Jones JR, Sutton PM *et al.* (1992) Occupational exposures in California wildland fire fighting. Am Ind Hyg Assoc J; 53: 69–76.

Musk AW, Peters JM, Bernstein L *et al.* (1982) Pulmonary function in firefighters: a six-year follow-up in the Boston Fire Department. Am J Ind Med; 3: 3–9.

Myers WR, Allender JR, Iskander W *et al.* (1988) Causes of in-facepiece sampling bias–I. Half-facepiece respirators. Ann Occup Hyg; 32: 345–59.

Myers WR, Zhuang Z, Nelson T. (1996) Field performance measurements of half-facepiece respirators–foundry operations. Am Ind Hyg Assoc J; 57: 166–74.

NIOSH. (2009) "Total Inward Leakage for Half-mask Air-purifying Respirators" http://www.cdc.gov/niosh/docket/archive/docket137.html. Accessed 17 November 2012.

Oestenstad RK, Bartolucci AA. (2010) Factors affecting the location and shape of face seal leak sites on half-mask respirators. J Occup Environ Hyg; 7: 332–41.

Oestenstad RK, Elliott LJ, Beasley TM. (2007) The effect of gender and respirator brand on the association of respirator fit with facial dimensions. J Occup Environ Hyg; 4: 923–30.

Oestenstad RK, Perkins LL. (1992) An assessment of critical anthropometric dimensions for predicting the fit of a half-mask respirator. Am Ind Hyg Assoc J; 53: 639–44.

Rengasamy S, Eimer BC. (2011) Total inward leakage of nanoparticles through filtering facepiece respirators. Ann Occup Hyg; 55: 253–63.

Rengasamy S, Eimer BC, Shaffer RE. (2009) Comparison of nanoparticle filtration performance of NIOSH-approved and CE-marked particulate filtering facepiece respirators. Ann Occup Hyg; 53: 117–28.

Rengasamy S, King WP, Eimer BC *et al.* (2008) Filtration performance of NIOSH-approved N95 and P100 filtering facepiece respirators against 4 to 30 nanometer-size nanoparticles. J Occup Environ Hyg; 5: 556–64.

Shaffer R, Rengasamy S. (2009) Respiratory protection against airborne nanoparticles: a review. J Nanoparticle Res; 11: 1661–72.

Shvedova AA, Kisin ER, Mercer R *et al.* (2005) Unusual inflammatory and fibrogenic pulmonary responses to single-walled carbon nanotubes in mice. Am J Physiol Lung Cell Mol Physiol; 289: L698–708.

Underwriters Laboratories Inc. (2010) Firefighter Exposure to Smoke Particulates. Available at http://www.ul.com/global/documents/offerings/industries/buildingmaterials/fireservice/WEBDOCUMENTS/EMW-2007-FP-02093.pdf. Accessed 15 November 2012).

Wong MH, Wu SC, Deng WJ *et al.* (2007) Export of toxic chemicals - a review of the case of uncontrolled electronic-waste recycling. Environ Pollut; 149: 131–40.

Zhuang Z, Coffey CC, Myers WR, Yang J, Campbell DL. (1998) Quantitative Fit-Testing of N95 Respirators: Part I-Method Development. J Int Soc Res Prot; 16: 11–24.

Downloaded from http://annhyg.oxfordjournals.org/ at CDC Public Health Library & Information Center on March 26, 2014